# Metal Complexes of New, Chiral $N_2O_2$ Tetradentate Ligands

**Ronald J. Cross,* Louis J. Farrugia, Paul D. Newman, Robert D. Peacock, and Diane Stirling**

Department of Chemistry, University of Glasgow, G12 8QQ, Scotland, UK

*Received February 19, 1998*

*N*,*N*′-Bis(2*R*-hydroxy-2*R*-phenylethyl)-*N*,*N*′-dimethyl-1*R*,2*R*-diaminocyclohexane, $H_2L1$, and *N*,*N*′-bis(2*S*-hydroxy-2*S*-methylethyl)-*N*,*N*′-dimethyl-1*R*,2*R*-diaminocyclohexane, $H_2L2$, have been synthesized from readily available chiral precursors. They coordinate as neutral tetradentate ligands to Ni(II) and Cu(II) ions, from which the thiocyanates $[M(H_2L)(NCS)_2]$ have been isolated and the structures of the $H_2L1$ complexes determined by single-crystal X-ray techniques. In the blue complex $[Ni(H_2L1)(NCS)_2]\cdot H_2O\cdot 2EtOH$, **1**, and green $[Cu(H_2L1)(NCS)_2]\cdot 0.5H_2O$, **2**, the neutral tetradentate ligands coordinate with the cis-α geometry with mutually cis N-bound thiocyanate groups, though the chiral ligands adopt a different stereochemistry in the two complexes. In **2**, the absolute configuration about the Cu(II) center is Δ, with the nitrogens possessing the S stereochemistry, whereas for the Ni(II) analogue, coordination gives the Λ isomer with the R configuration at the stereogenic nitrogens. Addition of $H_2L1$ or $H_2L2$ to Mn(II) in basic methanol solution results in rapid aerial oxidation. Δ-*cis*-α-$[Mn(L1)(OMe)_2]\cdot MeOH$, **3**, was isolated as black crystals from the reaction mixture after addition of 2 mol of NaOMe. The analogous complex with $(L2)^{2-}$ proved extremely hygroscopic and was not obtained in pure form. Colorless crystals of Λ-*cis*-α-$[MoO_2(L1)]$, **4**, were precipitated from a methanolic solution of $[MoO_2(acac)_2]$ and $H_2L1$. The analogous reaction with $H_2L2$ gave Δ-*cis*-α-$[MoO_2(L2)]$, **5**. Structures of **3**, **4**, and **5** are reported. The reactions of $H_2L1$ and $H_2L2$ with 1 mol equiv of $[Ti(OPr^i)_4]$ produced the complexes Δ-*cis*-α-$[Ti(L1)(OPr^i)_2]$ (white solid) and Λ-*cis*-α-$[Ti(L2)(OPr^i)_2]$ (colorless oil), structural assignments for which were made possible by analysis of their $^1$H NOE difference spectra. Thus the coordination of these tetradentate ligands is stereospecific, but the absolute configuration of the complexes formed (Δ or Λ) is dependent on the metal ion involved.

## Introduction

The pursuit of chiral ligands for application as auxiliaries in asymmetric catalysis is a primary concern of organic and inorganic chemists alike. Much of the current impetus is provided by the ever-increasing need for single enantiomers of the highest possible optical purity, exemplified by the requirements of the pharmaceutical industry.

Transition metals are often used as catalysts in such asymmetric transformations. Control of the stereochemistry about the active metal center is often paramount to the successful use of chiral ligands as auxiliaries. The presence of secondary isomers is often deleterious to the overall enantioselectivity of the processes. Our current interest is in asymmetric oxidation,[1,2] for which the most commonly used metals tend to be hard Lewis acids such as Ti(IV). We have thus set out to investigate a series of heterodonor ligands with donating groups designed for compatibility with these hard acids. One such class are the $N_2O_2$ tetradentate ligands discussed here.

Tetradentate $N_2O_2$ ligands of the Schiff-base type with sp$^2$ nitrogens and phenolic oxygens are ubiquitous.[3] The more flexible derivatives with sp$^3$ nitrogens and terminal alcohol(ate) donors have received comparatively little attention, although many examples of chiral bidentate N,O ligands have been reported,[4] in addition to $NO_2$ terdentates[5] and $NO_3$ tetradentates.[6] The utility of the latter two systems as asymmetric auxiliaries has been implied but not confirmed.[5,6]

The advantages associated with the use of $C_2$ symmetric ligands in enantioselective catalysis have been highlighted,[7] but examples are largely confined to mono- and bidentate systems. The tetradentate ligands $H_2L1$ and $H_2L2$ discussed herein were designed with the following features in mind: (*a*) they have $C_2$ symmetry; (*b*) the hard tertiary nitrogen and alcohol(ate) donors are compatible with high-oxidation level metal ions; (*c*) the central chelate unit incorporates the 1*R*,2*R*-diaminocyclohexane unit to enforce rigidity and encourage stereospecific coordination at octahedral centers such as Ti(IV); and (*d*) the chiral centers and attached substituents can readily be modified to allow performance comparisons with related complexes. This paper discusses the coordination chemistry of these ligands with hard ($Ti^{IV}$, $Mn^{IV}$, $Mo^{VI}$) and borderline ($Cu^{II}$, $Ni^{II}$) transition metal ions.

## Results and Discussion

**Syntheses.** The preparation of the ligands $H_2L1$ and $H_2L2$ is outlined in Scheme 1. The chiral precursors 1*R*,2*R*-diaminocyclohexane (*R,R*-chxn), *R*-styrene oxide, and *S*-propylene oxide are all available commercially, or may be obtained on a large

---

(1) Cross, R. J.; Farrugia, L. J.; Newman, P. D.; Peacock, R. D.; Stirling, D. *J. Chem. Soc., Dalton Trans.* **1996**, 4149−4150.

(2) Cross, R. J.; Farrugia, L. J.; Newman, P. D.; Peacock, R. D.; Stirling, D, *J. Chem. Soc., Dalton Trans.* **1996**, 4449−4458.

(3) Caligaris, M.; Randaccio, L. In *Comprehensive Coordination Chemistry*; Wilkinson, G., Gillard, R. D., McCleverty, J., Eds.; Pergamon: Elmsford, NY, 1987; Vol. 2, pp 715−738.

(4) See, for example, Soai, K.; Niwa, S. *Chem. Rev.* **1992**, *92*, 833−856. Blaser, H.-U. *Chem. Rev.* **1992**, *92*, 935−952.

(5) Barbaro, P.; Belderrain, T. R.; Bianchini, C.; Scapaci, G.; Masi, D. *Inorg. Chem.* **1996**, *35*, 3362−3368.

(6) Nugent, W. A.; Harlow, R. L. *J. Am. Chem. Soc.* **1994**, *116*, 6142−6148.

(7) Whitesell, J. K. *Chem. Rev.* **1989**, *89*, 1581−1590.

10.1021/ic980172l CCC: $18.00

**Scheme 1**

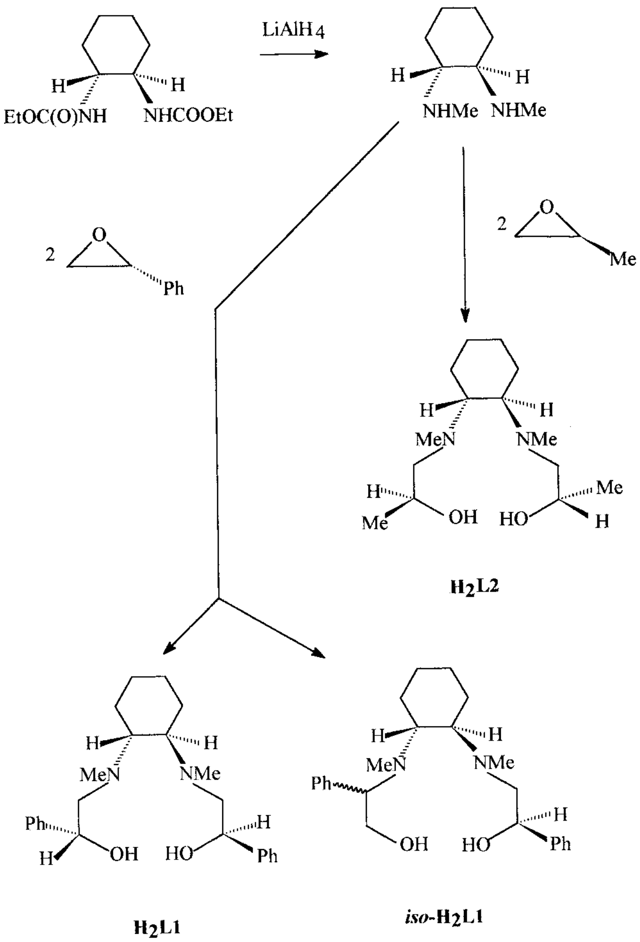

scale by established procedures.[8,9] Dimethylation of *R*,*R*-chxn was readily achieved following a modified procedure by Fujita and colleagues.[10] The ring-opening of *S*-propylene oxide occurs cleanly and with complete retention of configuration at the chiral carbon atoms to give $H_2L2$. The preparation of $H_2L1$ was complicated by the formation of a second isomer, *iso*-$H_2L1$, resulting from some nucleophilic attack at the phenyl-bearing carbon of the epoxide. This latter reaction led to a small reduction in the overall yield of $H_2L1$. The *iso*-$H_2L1$ would be expected to exist as a mixture of diastereoisomers if attack at *C*-Ph led to racemization at this center. The presence of two isomers was not evident from the $^1H$ and $^{13}C$ NMR spectra of *iso*-$H_2L1$, and it may be that this reaction occurs with a high degree of stereoselectivity (either for retention or inversion); this has not been investigated further in the present study.

In the absence of base, coordination of $H_2L1$ and $H_2L2$ to Ni(II) and Cu(II) occurred without loss of the hydroxyl protons but produced only intractable materials. When these reactions were followed by addition of $NCS^-$, however, crystalline complexes of composition $[M(NCS)_2(H_2L)]$ were isolated, of which $[Ni(NCS)_2(H_2L1)]$, **1,** and $[Cu(NCS)_2(H_2L1)]$, **2**, were obtained in suitable form for X-ray crystallographic analysis. No complexes of Ni(II) or Cu(II) with the dianionic ligands, $L^{2-}$, could be isolated, but the presence of such species was implicated in basic solution. Thus, for example, the color of a 1:1 Ni(II):ligand solution in 0.1 M NaOH is wine-red, typical of square planar $Ni^{II}$ complexes. Attempts to isolate the compounds led to intractable oils.

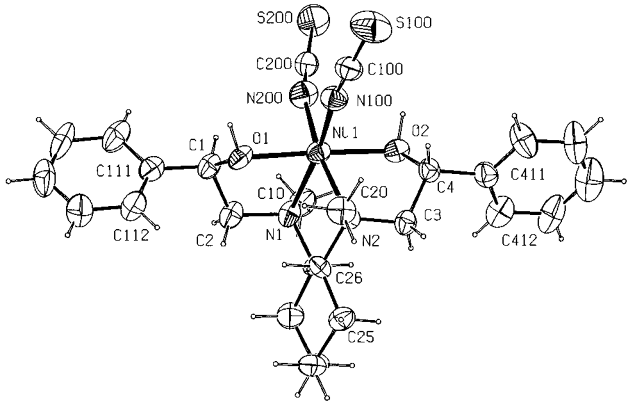

**Figure 1.** Molecular structure and atomic labeling scheme for $[Ni(NCS)_2(H_2L)]$, **1**, with thermal ellipsoids shown at the 30% probability level.

The addition of 1 mol equiv of $H_2L1$ to a methanolic solution of Mn(II) produced an immediate intense green-brown solution that became an opaque red-brown after adding 2 mole equiv of NaOMe. After leaving the reaction mixture overnight at −20 °C, lustrous black prisms of $[Mn(L1)(OMe)_2]$·MeOH, **3**, were isolated. An analogous procedure proved unsatisfactory for $H_2L2$, where only mixed complexes of an ill-defined character were obtained. In both cases the complexes formed initially were extremely hygroscopic solids and these were not examined further.

Upon leaving methanolic solutions of $[MoO_2(acac)_2]$ and 1 mol equiv of the appropriate ligand $H_2L1$ or $H_2L2$ to stand at room temperature, the complexes $[MoO_2(L)]$ (**4**, L = L1, and **5**, L = L2) formed readily as colorless, crystalline solids. For $[MoO_2(L1)]$, care must be exercised not to leave the solution for too long before isolation, as there was a tendency for the product to decompose to a dark blue solid.

The reaction of equimolar quantities of $H_2L1$ or $H_2L2$ with $[Ti(OPr^i)_4]$ in dichloromethane yielded various products depending on the reaction time. When solutions of $[Ti(OPr^i)_4]$ and $H_2L1$ were stirred together for 1−2 h, a mixture of two isomers, both of $C_2$ symmetry, were observed by NMR spectroscopy after removal of the reaction solvent. After leaving the reaction mixture for several days, however, a single isomer of $[Ti(L1)(OPr^i)_2]$ was obtained as a white solid. The $[Ti(L2)(OPr^i)_2]$ system behaved similarly, although the mixture obtained after low reaction times appeared somewhat more complicated. As before, however, this reaction ultimately gave a single isomer of $[Ti(L2)(OPr^i)_2]$, this time as a colorless oil, after allowing the reaction to continue to completion.

**Crystal Structures of 1, 2, 3, 4 and 5.** The molecular structures of **1**, **2**, **3**, **4**, and **5** are shown in Figures 1−5, with salient bond lengths and angles summarized in Tables 1 and 2. All the complexes are six-coordinate, pseudo-octahedral, with the monodentate ligands cis and the tetradentate ligand coordinated with the α-geometry, as defined by the mutually trans terminal alcohol(ate) donors. The coordination spheres thus approximate to $C_2$ symmetry.

For the Ni(II) complex, **1**, the M−L bond lengths are all quite similar at 2.1 ± 0.1 Å. The $Mn^{IV}$−L bond lengths in **3** are less regular, and the Cu(II) and Mo(VI) systems have large disparities in their M−L bond lengths. The $d^9$ copper(II) ion in **2** shows the expected Jahn−Teller distortion along one of the nominal

---

[8] Galsbøl, F.; Steenbøl, P.; Sørencen, B. S. *Acta Chem. Scand.* **1972**, *26*, 3605−3611.

[9] Fallis, I. A.; Farrugia, L. J.; MacDonald, N. M.; Peacock, R. D. *J. Chem. Soc., Dalton Trans.* **1993**, 2759−2763.

[10] Kashiwabara, K.; Hanaki, K.; Fujita, J. *Bull. Chem. Soc. Jpn.* **1980**, *53*, 2275−2280.

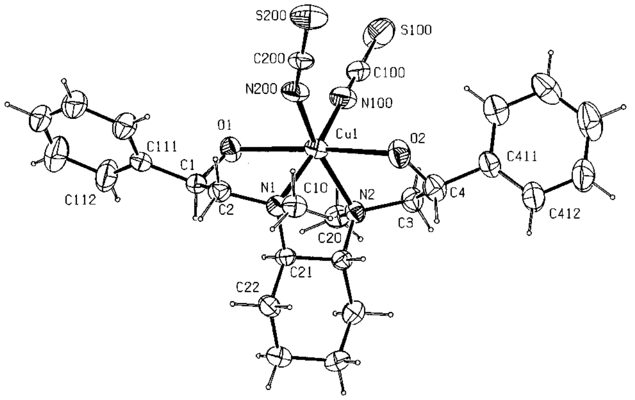

**Figure 2.** Molecular structure and atomic labeling scheme for [Cu(NCS)$_2$(H$_2$L)], **2**, with thermal ellipsoids shown at the 30% probability level.

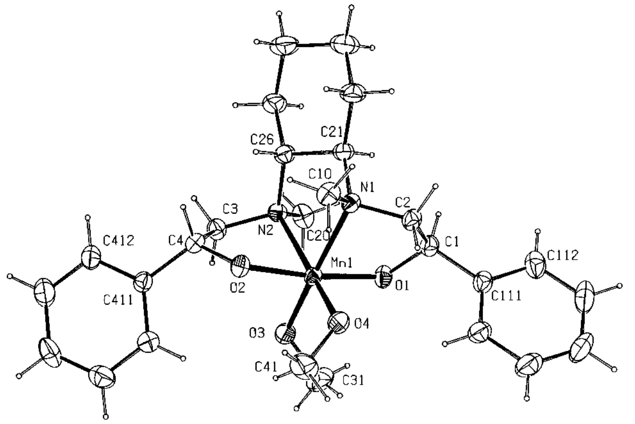

**Figure 3.** Molecular structure and atomic labeling scheme for [Mn(L1)(OMe)$_2$], **3**, with thermal ellipsoids shown at the 30% probability level.

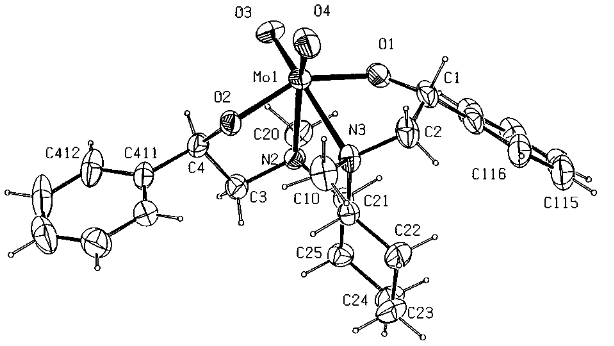

**Figure 4.** Molecular structure and atomic labeling scheme for [MoO$_2$(L1)], **4**, with thermal ellipsoids shown at the 30% probability level.

octahedral axes, in this case along the O−Cu−O axis with the Cu−O vectors being elongated to >2.4 Å. In the molybdenum complexes **4** and **5** the Mo═O bonds are characteristically short (~1.7 Å), whereas the Mo−N bonds are lengthened to >2.4 Å as a consequence of their position trans to these strongly $\sigma$- and $\pi$-bonding functionalities.[11] The metal−nitrogen bonds in the Cu, Ni, and Mn complexes are all quite similar, but their M−O bond lengths span a wide range, from the Jahn−Teller elongation observed in **2** to the shortened Mn$^{IV}$−O bonds of **3**. This shortening is presumably a consequence of the better donor properties of the alcoholate groups compared with their protonated forms, coupled with the higher oxidation level of the metal. The stabilization of the Mn(IV) state by alkoxide donors has been commented on previously.[12]

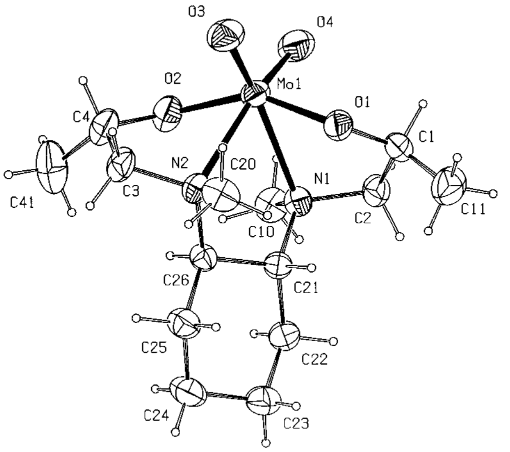

**Figure 5.** Molecular structure and atomic labeling scheme for [MoO$_2$(L2)], **5**, with thermal ellipsoids shown at the 30% probability level.

**Table 1.** Metal−Ligand Bond Lengths (Å) for Compounds **1**, **2**, **3**, **4**, and **5**

| | **1**<br>(M = Ni) | **2**<br>(M = Cu) | **3**<br>(M = Mn) | **4**<br>(M = Mo) | **5**<br>(M = Mo) |
|---|---|---|---|---|---|
| M−N1 | 2.180 (6) | 2.053 (4) | 2.127 (3) | 2.424 (3) | 2.400 (2) |
| M−N2 | 2.128 (6) | 2.085 (4) | 2.125 (3) | 2.380 (3) | 2.382 (2) |
| M−O1 | 2.077 (5) | 2.411 (3) | 1.863 (2) | 1.941 (3) | 1.933 (2) |
| M−O2 | 2.087 (5) | 2.402 (3) | 1.897 (2) | 1.950 (3) | 1.940 (2) |
| M-NCS | 2.024 (8) | 1.982 (5) | | | |
| | 2.027 (7) | 1.983 (5) | | | |
| Mn−OMe | | | 1.826 (2) | | |
| | | | 1.838 (2) | | |
| Mo═O | | | | 1.696 (3) | 1.706 (2) |
| | | | | 1.699 (3) | 1.707 (2) |

**Table 2.** Selected Bond Angles (deg) for **1**, **2**, **3**, **4**, and **5**

| | **1**<br>(M = Ni) | **2**<br>(M = Cu) | **3**<br>(M = Mn) | **4**<br>(M = Mo) | **5**<br>(M = Mo) |
|---|---|---|---|---|---|
| N1−M−N2 | 83.1 (2) | 84.53 (14) | 82.31 (10) | 73.43 (10) | 74.53 (8) |
| N1−M−O1 | 79.4 (2) | 76.47 (12) | 81.08 (9) | 74.24 (11) | 71.33 (8) |
| N1−M−O2 | 98.3 (2) | 98.88 (14) | 94.47 (9) | 84.19 (11) | 85.26 (9) |
| O1−M−O2 | 177.3 (2) | 175.34 (12) | 172.92 (10) | 150.80 (11) | 150.69 (9) |
| N2−M−O1 | 98.3 (2) | 104.26 (13) | 93.71 (10) | 80.98 (11) | 84.40 (8) |
| N2−M−O2 | 79.9 (2) | 74.78 (14) | 80.19 (9) | 74.05 (10) | 72.24 (8) |

The bite angles (Table 2) of the N−M−O rings in the complexes **1** and **3** (where N and O form a chelate arm) are ~80°, whereas a slight compression to ~76° is observed in **2** as a consequence of the longer Cu−O bonds resulting from the Jahn−Teller distortion. The angles defined at the metal by the nitrogens of one N,O chelate ring and the oxygen of the opposing chelate [e.g., angle N(1)−Ni−O(2) in **1**] are expanded to ~100°, the exact values being dependent on the M−O and M−N lengths involved. The N−M−N angles, on the other hand, are largely invariant at ~83° for each of these three complexes.

The bond angles at molybdenum in the complexes [MoO$_2$(L1)] and [MoO$_2$(L2)] (**4** and **5**) reveal large distortions from octahedral geometry. The longer Mo−N distances and fixed bite angles of the ligands produce reduced N−Mo−N angles of <75°. The O(1)−Mo−O(2) trans angle is reduced to ~150°, and all angles between the tetradentate donors are compressed relative to the equivalent values in **1**, **2**, and **3**. These features are characteristic of such systems containing a tetradentate ligand and the *cis*-MoO$_2^{2+}$ core.[11]

---

(11) Hinshaw, C. J.; Peng, G.; Singh, R.; Spence, J. T.; Enemark, J. H.; Bruck, M.; Kristofski, J.; Merbs, S. L.; Ortega, R. B.; Wexler, P. A. *Inorg. Chem.* **1989**, *28*, 4483−4491.

(12) Kessissoglou, D. P.; Li, X.; Butler, W. M.; Pecoraro, V. L. *Inorg. Chem.* **1987**, *26*, 2487−2492.

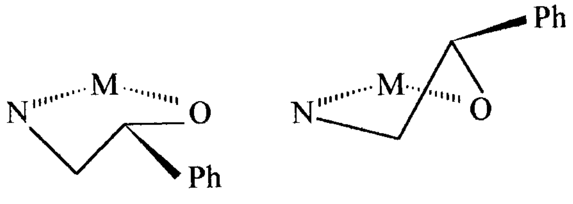

**6(a)** **6(b)**

**Figure 6.** Conformations of chelate arms.

The four stereogenic carbons have the absolute configurations *R,R,R,R* in the complexes of ($H_2$)L1 or L1, and *S,R,R,S* in the L2 complex, **5**, as defined by the choice of the starting diamine and the epoxide. The central chelate adopts the $\lambda$ conformation in all the complexes as determined by the chirality of the diaminocyclohexane unit. However, the stereogenic nitrogens do not have the same stereochemistry through the series. In **1** and **4** the two nitrogens adopt the *R,R* configuration, whereas in **2**, **3**, and **5** they are *S,S*. In both forms the N-bonded methyls are mutually trans. This relative inversion between the **1**, **4** pair and the **2**, **3**, **5** triad alters the absolute configuration about the metal center. In the Ni(II)(H2L1) and Mo(VI)(L1) complexes this is Λ, but for the Cu(II)(H2L1), Mn(IV)(L1), and Mo(VI)-(L2) complexes it is Δ. It appears, therefore, that although the coordination of $H_2L/L^{2-}$ is stereospecific, the absolute configuration is dependent on the metal ion (vide infra).

The conformation of the terminal N,O chelates is controlled by the combined configurations of the carbon and nitrogen centers of the rings. In the Δ forms of ($H_2$)L1, where the stereochemistry is *R*(C), *S*(N), the terminal chelates have the pseudoenvelope conformation shown in Figure 6(a), whereas the *R*(C), *R*(N) combination in the Λ isomers gives the geometry shown in Figure 6(b). The methyl groups have a more axial projection with respect to the $N_2X_2$ plane in the Δ form than in the Λ isomer. The distinction between the two chelates is the consequence of the phenyl group tending to adopt a more-or-less equatorial disposition; it achieves this in both isomers, although it is more axial in the Δ diastereoisomer. Because of the differing conformations of the rings in the pairs of complexes **1**, **4** and **2**, **3**, the aromatic groups have a different orientation with respect to the cyclohexane ring and the monodentate secondary ligands. For **1** and **4** the aromatic groups project toward the cyclohexane ring and may be described as being endo disposed. In **2** and **3** the disposition is toward the monodentate ligands and, as such, is described as the exo form. The methylene and methine hydrogens of the terminal chelates are not equivalent in these two forms. This has implications for the identification by NMR spectroscopy of the diamagnetic titanium species discussed below. The unique *S*(C), *S*(N) configuration in [$MoO_2$(L2)], **5**, gives a terminal chelate that is a true envelope with endo-disposed pseudoequatorial C-methyls.

**NMR Studies.** $^1$H and $^{13}$C NMR details of $H_2$L1, $H_2$L2, the molybdenum compounds **4** and **5**, and titanium compounds [Ti-(L1)($OPr^i$)$_2$] and [Ti(L2)($OPr^i$)$_2$] are summarized in Table 3. As noted for related systems,[5,6] the proton and carbon-13 resonances of the ligands tend to be shifted downfield on coordination. The NMR spectra of the Ti(IV) complexes are those of the final, presumably thermodynamically favored, isomers. Other isomers were present early in the reaction sequences. Thus when solutions of [Ti($^i$PrO)$_4$] and $H_2$L1 were mixed, and the resultant complex isolated after 1−2 h, two isomers were observed. When the reaction was allowed to proceed for more than 2 days, however, only one of them remained. A similar pattern was observed for the $L2^{2-}$ system, but in this case additional species were present early in the reaction, making the interpretation of the spectra very complicated. This system also later stabilized at a single isomer.

The oxo groups in [$MoO_2$(L)] are known to have a strong preference for being mutually cis. Therefore, upon dissolution, only two isomers (excluding optical antipodes) are expected for these complexes, namely the cis-α and cis-*β* forms (Figure 7). The $^{13}$C NMR spectra of [$MoO_2$(L1)] and [$MoO_2$(L2)] contain 10 and seven signals, respectively, compatible with the presence of single species of $C_2$ symmetry within the solutions. Thus, the possibility of either of the complexes having the cis-*β* ($C_1$) geometry is precluded.

Having established that the [$MoO_2$(L)] complexes are cis-α, it is possible to deduce the absolute configuration by close inspection of the NMR spectra, in particular the NOE difference spectra. By virtue of its very simple $^1$H spectrum, [$MoO_2$(L2)] will be analyzed first. The isolation and crystallographic characterization of the Δ-cis-α isomer of $MoO_2$(L2) would strongly suggest that such a geometry be retained in solution. Examination of the NOE difference spectra would appear to confirm this. When the methine protons in the terminal chelates are irradiated ($\delta$ = 4.78 ppm), the only resonances showing positive NOE enhancements are those of the vicinal neighbors Hb ($\delta$ = 3.47 ppm) and the geminal methyl groups ($\delta$ = 1.31 ppm): the remaining vicinal partners Hc ($\delta$ = 2.81 ppm) show small negative NOEs as expected (see diagram below).

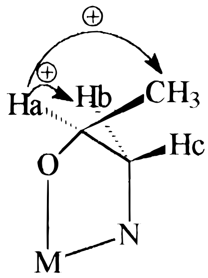

Apart from the positive enhancement of the Ha resonance, irradiation of the C-methyl protons leads to large positive NOEs at Hd ($\delta$ = 2.57 ppm), He ($\delta$ = 2.05 ppm), and Hc, as shown in the figure below, with a small negative effect at Hb.

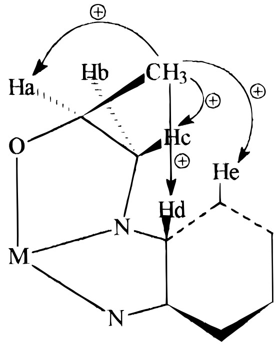

Thus the C-methyls must reside over the central chelate. This is only possible when the complex has the Δ configuration, and it is concluded that Δ-*cis*-α-[$MoO_2$(L2)] retains its stereochemistry in solution.

As the stereogenic carbons α to the alcoholate oxygens in L1 possess the opposite configuration (*R*) relative to L2 (*S*), the observation of similar NOE enhancements in the spectra of $MoO_2$(L1) with respect to $MoO_2$(L2) would be deemed indicative of the opposite configuration about the metal. That is, if the methine protons Ha only exert a positive NOE influence

**Table 3.** Selected $^1$H and $^{13}$C NMR Data for $H_2L1$, $H_2L2$, and Their Complexes with Mo(VI) and Ti(IV)

| | compound | | | | | |
|---|---|---|---|---|---|---|
| assignment | $H_2L1$ | $H_2L2$ | $MoO_2(L1)$ | $MoO_2(L2)$ | $Ti(L1)(^iPrO)_2$ | $Ti(L2)(^iPrO)_2$ |
| Ha | 4.85dd<br>(*10,12*) | 3.74m | 5.59dd<br>(*11,5*) | 4.78m | 5.42dd<br>(*10,5*) | 4.51m |
| Hb | 2.72dd<br>(*14,10*) | 2.13dd<br>(*13,9*) | 2.74dd<br>(*13,11*) | 3.47dd<br>(*12,10*) | 3.14dd<br>(*12,10*) | 2.50dd<br>(*12,11*) |
| Hc | 2.34dd<br>(*14,2*) | 2.61dd<br>(*13,3*) | 2.97dd<br>(*13,5*) | 2.81dd<br>(*12,3*) | 3.02dd<br>(*12,5*) | 2.93dd<br>(*13,4*) |
| N−$CH_3$ | 2.57s | 2.24s | 3.21s | 2.66s | 2.52s | 2.69s |
| $C_1$ | 71.6 | 66.0 | 85.7 | 76.6 | 75.9 | 73.5 |
| $C_2$ | 59.8 | 62.2 | 62.3 | 63.0 | 65.4 | 62.9 |
| N−$CH_3$ | 41.1 | 37.1 | 46.1 | 40.8 | 39.5 | 49.1 |
| $C_1$−$CH_3$ | | 20.4 | | 26.7 | | 23.3 |

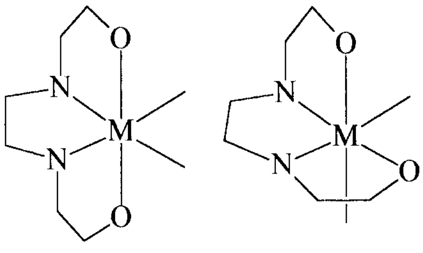

*cis*-α *cis*-β

**Figure 7.** Possible conformations of *cis*-[$MoO_2$(L)].

on their vicinal partners Hb (excluding any obvious effect at the phenyl protons) and no other resonance, then they must reside away from the central chelate. The major NOE effects observed in $MoO_2$(L1) are outlined below.

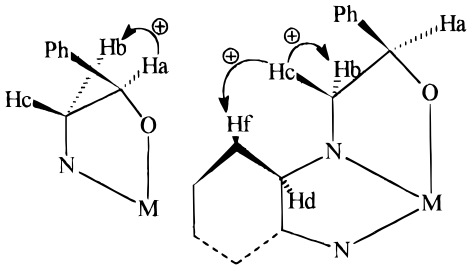

In addition to those enhancements indicated, irradiation of the Hb resonance produces a positive NOE for the N-methyl protons, confirming the configuration as $\Lambda$. Therefore $\Lambda$-*cis*-α-[$MoO_2$(L1)] retains its stereochemical integrity on dissolution also.

The $^1$H and $^{13}$C spectra of [Ti($L_2$)($^i$PrO)$_2$] and [Ti(L1)($^i$PrO)$_2$] are, like the molybdenum complexes already discussed, indicative of the presence of a two-fold symmetry element within the complexes: as any trans form is energetically disfavored, the stereochemistry is defined as α-cis. The patterns observed in the NOE difference spectra of [$MoO_2$(L2)] are not manifest in those for [Ti(L2)($^i$PrO)$_2$]: most notably, irradiation of the C-methyl protons in the titanium complex leads to positive NOEs for the Ha and Hc resonances only. The methyl groups must, therefore, be residing away from the central chelate and the configuration is assigned as $\Lambda$. Similarly, the spectra of [Ti(L1)($^i$PrO)$_2$] are not concordant with those of the molybdenum complex of the same ligand, with the observed NOEs being consistent with the $\Delta$ configuration for this Ti(IV) complex.

**Table 4.** Electronic and CD Spectroscopic Data[a]

| complex | $\lambda$/nm ($\epsilon$/dm$^3$ mol$^{-1}$ cm$^{-1}$) | $\lambda$/nm ($\delta\epsilon$/dm$^3$ mol$^{-1}$ cm$^{-1}$) |
|---|---|---|
| $\Lambda$-cis-α-[Ni($H_2L1$)$(NCS)_2$]$H_2O$•2EtOH | 602 (20)<br>380 (37) | 680 (+0.025)<br>580 (+0.042)<br>400 (+0.045) |
| $\Delta$-cis-α-[Cu($H_2L1$)$(NCS)_2$]•0.5$H_2O$ | 694 (119) | 640 (−0.326) |
| $\Lambda$-cis-α-[Ni($H_2L2$)$(NCS)_2$]•0.5$H_2O$ | 615 (21)<br>381 (36) | 600 (+0.031)<br>425 (+0.050) |
| $\Lambda$-cis-α-[Cu($H_2L2$)$(NCS)_2$]•EtOH | 696 (141) | 575 (+0.186) |
| $\Delta$-cis-α-[Mn(L1)$(OMe)_2$]•MeOH | 511 (299) | 670 (+0.088)<br>517 (−0.396) |

[a] Recorded in MeCN, except for the Mn(IV) compound, which was recorded in $CH_2Cl_2$.

**Electronic and Chiroptical Properties.** The UV−vis and CD spectral features of the Ni(II), Cu(II), and Mn(IV) complexes are summarized in Table 4. The low extinction coefficients of the nickel(II) and copper(II) complexes are consistent with a d-to-d origin and approximately octahedral chromophores. By contrast, the large $\epsilon$ values of the Mn$^{IV}$ system are suggestive of a charge-transfer origin for the visible absorption bands. The CD spectra of [Ni($H_2L1$)$(NCS)_2$] and [Ni($H_2L2$)$(NCS)_2$] are similar, with positive manifolds throughout the visible range. The two spin-allowed transitions of $O_h$ parentage are $^3A_{2g} \rightarrow {}^3T_{1g}$ and $^3A_{2g} \rightarrow {}^3T_{1g}(P)$. It is clear from the CD spectra of [Ni($H_2L1$)$(NCS)_2$] that the lower energy transition has two components reflecting the lack of degeneracy in the excited state, as is necessarily the case for these strictly $C_2$ complexes.[13] [Ni($H_2L1$)$(NCS)_2$] is assumed to adopt the same absolute configuration in solution as determined in the solid state ($\Lambda$), and the similar CD spectrum of the analogous complex with $H_2L2$ would suggest that this also has the $\Lambda$ configuration.

Unlike the Ni(II) systems, the [Cu($H_2L1$)$(NCS)_2$]/[Cu($H_2L2$)$(NCS)_2$] pair have disparate CD spectra. For the former complex, the visible CD spectrum is dominated by a single negative peak, whereas for the $H_2L2$ analogue a single positive maximum is observed. It seems likely that [Cu($H_2L2$)$(NCS)_2$] adopts the "enantiomeric" configuration with respect to [Cu($H_2L1$)$(NCS)_2$]; the latter is believed to be $\Delta$ in accord with its X-ray molecular structure, so we assign the former as $\Lambda$.

A short investigation of the oxidation catalytic properties of some of these compounds revealed that although both of the

---

(13) The following discussion presumes the *cis*-α form is predominant in solution.

titanium complexes Δ-*cis*-α-[Ti(L1)($OPr^i$)$_2$] and Λ-*cis*-α-[Ti(L2)($OPr^i$)$_2$] are efficient catalysts for the $Bu^tOOH$ oxidation of prochiral sulfides to sulfoxides, only the former confers a small but significant enantiomeric excess (15%) on the product.

## Experimental Section

NMR spectra were recorded on a Bruker AM 200 spectrometer operating in the Fourier transform mode. IR spectra were recorded on a Phillips PU 9800 spectrometer and UV−Vis spectra on a Perkin-Elmer Lambda 9. CD spectra were recorded on home-built apparatus. Microanalyses were carried out by Glasgow University Chemistry Department microanalytical service.

***N,N′*-Dimethyl-1*R*,2*R*-diaminocyclohexane.** 1*R*,2*R*-bis(ethoxycarbonylamino)cyclohexane[10] (7.3 g) in THF (50 cm$^3$) was added dropwise to a stirred slurry of $LiAlH_4$ (8 g) in THF (150 cm$^3$) under nitrogen. The mixture was refluxed with stirring overnight, cooled to 0 °C, and carefully hydrolyzed by the dropwise addition of $H_2O$ (30 cm$^3$). After stirring for a further 2 h, the mixture was filtered and the aluminate cake washed with hot THF (300 cm$^3$). The filtrate and washings were taken to dryness in vacuo, and the residue partitioned between diethyl ether and 6 M aqueous NaOH. The organic phase was dried ($MgSO_4$), filtered, and the solvent removed to give a colorless oil that crystallized on standing. Yield = 60%.

***N,N′*-Bis(2*R*-hydroxy-2*R*-phenylethyl)-*N,N′*-dimethyl-1*R*,2*R*-diaminocyclohexane ($H_2L1$).** A mixture of *N,N′*-dimethyl-1*R*,2*R*-diaminocyclohexane (2 g, 14.1 mmol), prepared as above, and *R*-styrene oxide (3.34 g, 28.2 mmol) in EtOH (50 cm$^3$) was left in a stoppered flask for 7 days at room temperature. Removal of the solvent yielded an orange oil that gave two spots by TLC (alumina, toluene:EtOAc:$Et_3N$ 50:45:2.5; $R_f = 0.65_{\text{minor}}$ and $0.80_{\text{major}}$) indicating the presence of two isomers. Dry-column chromatography ($SiO_2$, 4.5 × 140 cm$^3$) using ethyl acetate in toluene (10% to 45% in 5% increments for fractions 1−8) and then 0.5% to 5% $Et_3N$ in 1:1 toluene:ethyl acetate (0.5% increments for fractions 9−18) gave both isomers in pure form. The major product, $H_2L1$, was obtained as a slightly yellow viscous oil (70% yield), and the minor product, identified as *N*-(2*R*-hydroxy-2*R*-phenylethyl)-*N′*-(2-hydroxy-1-phenylethyl)-*N,N′*-dimethyl-1*R*,2*R*-diaminocyclohexane, *iso*-$H_2L1$, was recovered as a white solid (15% yield). **$H_2L1$**: Calcd for $C_{24}H_{34}N_2O_2$: C, 75.33; H, 8.97; N, 7.32. Found: C, 75.2; H, 9.9; N, 7.3.

***N,N′*-Bis(2*S*-hydroxy-2*S*-methylethyl)-*N,N′*-dimethyl-1*R*,2*R*-diaminocyclohexane ($H_2L2$).** The reaction was repeated as detailed for $H_2L1$ above but replacing the *R*-styrene oxide by *S*-propylene oxide (10% excess), and reducing the reaction time to 5 days. Removal of the solvent gave the product as a golden yellow oil, yield = 100%. Calcd for $C_{14}H_{30}N_2O_2$: C, 66.05; H, 11.72; N, 10.84. Found: C, 64.7; H, 11.6; N, 10.5.

**Λ-*cis*-α-[Ni($H_2L1$)($NCS)_2$]·$H_2O$·2EtOH.** To a stirred solution of nickel(II) nitrate hexahydrate (0.31 g, 1.05 mmol) in EtOH (15 cm$^3$) was added $H_2L1$ (0.40 g, 1.05 mmol), giving a green solution. Potassium thiocyanate (0.21 g, 2.10 mmol) in $H_2O$ (5 cm$^3$) was then added, whereupon the solution immediately turned blue, and a pale blue precipitate subsequently formed. This was obtained by filtration, washed with $H_2O$ and then dry $Et_2O$, and air-dried. The filtrate was left to stand overnight, giving blue prisms suitable for X-ray analysis. Total yield = 350 mg (50%). Calcd for $C_{27}H_{39}N_4O_{3.5}S_2Ni$ (the compound lost weight corresponding to 1.5 EtOH before combustion): C, 53.83; H, 6.54; N, 9.30. Found: C, 53.4; H, 6.5; N, 9.3.

**Λ-*cis*-α-[Ni($H_2L2$)(NCS)2]·0.5$H_2O$.** This was prepared as detailed for the $H_2L1$ derivative above. The pale blue solid precipitated after standing for 2 days. Yield = 400 mg (70%). Calcd for $C_{16}H_{31}N_4O_{2.5}S_2Ni$: C, 43.46; H, 7.08; N, 12.67. Found: C, 43.5; H, 7.3; N, 12.4.

**Δ-*cis*-α-[Cu($H_2L1$)($NCS)_2$]·0.5$H_2O$.** To a stirred solution of copper(II) nitrate trihydrate (0.253 g, 1.05 mmol) in EtOH (20 cm$^3$) was added $H_2L1$ (0.40 g, 1.05 mmol). During the addition the color deepened from pale to dark blue. A solution of KSCN (0.21 g, 2.10 mmol) in $H_2O$ (5 cm$^3$) was added, giving a dark green solution from which a gray-green solid quickly precipitated. This was filtered off and discarded. The turquoise-colored filtrate was left for several hours, whereupon a green-blue crystalline solid was precipitated. This was filtered off, washed sparingly with 1:1 $H_2O$:EtOH, and air-dried. Further product was obtained by leaving the filtrate to stand. The solids were recrystallized from EtOH to give elongated green prisms suitable for X-ray analysis. Yield = 0.30 g (50%). Calcd for $C_{26}H_{35}N_4O_{2.5}S_2Cu$: C, 54.67; H, 6.19; N, 9.81. Found: 54.3; H, 6.3; N, 9.5.

**Λ-*cis*-α-[Cu($H_2L2$)($NCS)_2$]·EtOH.** To a solution of copper(II) nitrate trihydrate (0.158 g, 6.5 × 10$^{-4}$ mol) in MeOH (5 cm$^3$) was added $H_2L2$ (0.25 g, 6.25 × 10$^{-4}$ mol), giving a deep blue solution. KSCN (0.127 g, 1.31 mmol) was added as a solid to the stirred solution, whereupon the color changed to deep green. Precipitated $KNO_3$ was filtered off, and the filtrate taken to near dryness in vacuo. The residue was partitioned between $CH_2Cl_2$ and $H_2O$, the organic phase isolated and dried ($MgSO_4$), and the solvent then removed in vacuo to give the product as a dark green solid. Calcd for $C_{18}H_{36}N_4O_3S_2Cu$: C, 44.65; H, 7.51; N, 11.58. Found, C, 45.0; H, 7.1; N, 11.7. Yield = 0.15 g.

**Δ-*cis*-α-[Mn(L1)($OMe)_2$]·MeOH.** Anhydrous manganese(II) chloride (0.66 g, 5.2 mmol) was dissolved with stirring in predried MeOH (25 cm$^3$) in the absence of atmospheric $H_2O$. A solution of $H_2L1$ (2.0 g, 5.2 mmol) in MeOH (15 cm$^3$) was added, producing an immediate opaque green-brown solution. Sodium ethoxide (0.76 g, 10.4 mmol) was then added as a solid, causing a change to red-brown and the formation of a slight precipitate, which soon redissolved. After stirring for a further 1 h, the mixture was filtered, and the filtrate left at −20 °C overnight. The resultant black crystals were filtered off, washed sparingly with ice-cold MeOH, and air-dried. A second crop was obtained on further cooling the filtrate. Total yield = 0.80 g (29%). Calcd for $C_{27}H_{41}N_2O_5Mn$: C, 61.34; H, 7.83; N, 5.30. Found: C, 60.8; H, 7.6; N, 5.3.

**Λ-*cis*-α-[$MoO_2$(L1)].** [$MoO_2$(acac)$_2$] was dissolved in MeOH (10 cm$^3$) with warming, filtered, and to the filtered solution was added $H_2L1$ in MeOH (5 cm$^3$). The clear, colorless solution was left to stand overnight, whereupon colorless prisms of the title complex were obtained. These were filtered off, washed sparingly with MeOH, and air-dried. A second crop was obtained on leaving the filtrate and washings to stand. Yield = 50%. Calcd for $C_{24}H_{32}N_2O_4Mo$: C, 56.79; H, 6.37; N, 5.52. Found, C, 56.7; H, 6.3; N, 5.4.

**Δ-*cis*-α-[$MoO_2$(L2)].** The compound was prepared exactly as detailed for the analogous complex with L1, above, substituting $H_2L2$ for $H_2L1$. Colorless prisms of the product precipitated overnight. Yield = 80%. Calcd for $C_{14}H_{28}N_2O_4Mo$: C, 43.86; H, 7.38; N, 7.31. Found: 43.7; H, 7.4; N, 7.3.

**Δ-*cis*-α-[Ti(L1)($OPr^i$)$_2$].** To a stirred solution of titanium(IV) isopropoxide (0.223 g, 7.8 × 10$^{-4}$ mol) in dichloromethane (15 cm$^3$) under nitrogen was added a solution of $H_2L1$ (0.300 g, 7.8 × 10$^{-4}$ mol) in dichloromethane (10 cm$^3$). The solution was stirred for 3 days, then pumped to dryness to give the product as a white solid. Yield = 100%. Calcd for $C_{30}H_{46}N_2O_4Ti$: C, 65.91; H, 8.50; N, 5.13. Found: C, 65.8; H, 8.6; N, 5.0.

**Λ-*cis*-α-[Ti(L2)($^iPrO$)$_2$].** This was prepared as detailed for L1 above but using $H_2L2$. The desired complex was obtained as a colorless, hygroscopic oil. Yield = 100%.

## Experimental Details of Structure Determinations

Details of data collection procedures and structure refinements for all five crystallographic studies are given in Table 5. Single crystals of suitable size were attached to a glass fiber using acrylic resin, and mounted on a goniometer head in a general position. Data were collected in bisecting mode on an Enraf-Nonius TurboCAD4 diffractometer, running under CAD4-Express software, and using graphite monochromated X-radiation ($\lambda$ = 0.71073 Å). All data sets were collected at ambient temperature (∼20 °C). Precise unit cell dimensions were determined by refinement of the setting angles of 25 high-angle reflections that were flagged during data collection. Standard reflections were measured every 2 h during data collection, and an interpolated correction was applied to the reflection data where necessary. Lorentz polarization corrections were then applied to the reflection data. For complexes **2** and **4** a semiempirical absorption correction ($\psi$-scans) was applied, whereas for complex **5** an absorption correction by the method of Stuart and Walker[14] was applied. For complexes **1** and **3**

**Table 5.** Experimental Details of the Crystallographic Studies

| | **1** | **2** | **3** | **4** | **5**[b] |
|---|---|---|---|---|---|
| compound formula | $C_{30}H_{48}N_4NiO_5S_2$ | $C_{26}H_{34}CuN_4O_2S_2$ | $C_{27}H_{42}MnN_2O_5$ | $C_{24}H_{32}MoN_2O_4$ | $C_{14}H_{28}MoN_2O_4$ |
| compound color | blue | green | black | colorless | colorless |
| $M_r$ | 667.55 | 562.23 | 529.57 | 508.46 | 384.32 |
| space group | $P2_12_12_1$ | $P2_12_12_1$ | $P2_1$ | $P2_12_12_1$ | $P2_12_12_1$ |
| crystal system | orthorhombic | orthorhombic | monoclinic | orthorhombic | orthorhombic |
| $a$/Å | 12.1771(9) | 12.6001(8) | 8.2617(6) | 12.0939(9) | 8.4076(4) |
| $b$/Å | 13.230 (2) | 15.533(2) | 16.3890(11) | 13.2977(8) | 13.4180(7) |
| $c$/Å | 21.7666 (14) | 16.077(2) | 10.3526(7) | 14.259(2) | 15.0054(9) |
| $\beta$/deg | 90 | 90 | 96.114(6) | 90 | 90 |
| $V$/Å$^{-3}$ | 3506.7 (6) | 3146.7(6) | 1393.8(2) | 2293.1 | 1692.8(2) |
| $\theta$ range for cell | 9.4−19.2 | 17.6−20.9 | 17.6−20.9 | 17.5−20.9 | n/a |
| $Z$ | 4 | 4 | 2 | 4 | 4 |
| $D_{calc}$/g cm$^{-3}$ | 1.264 | 1.187 | 1.262 | 1.473 | 1.508 |
| $F$(000) | 1424 | 1180 | 566 | 1056 | 800 |
| $\mu$(Mo Kα)/cm$^{-1}$ | 7.13 | 8.53 | 5.11 | 6.04 | 7.91 |
| scan mode | $\bar{\omega}/2\theta$ | $\bar{\omega}/2\theta$ | $\bar{\omega}/2\theta$ | $\bar{\omega}/2\theta$ | $\omega/2\theta$ |
| $\omega$ scan angle/deg | 0.91+ 0.47 tan($\theta$) | 0.59 + 0.50 tan($\theta$) | 0.68 + 0.45 tan($\theta$) | 0.64 + 0.41 tan($\theta$) | n/a |
| $\theta$ range/deg | 2.5−25.0 | 2.4−25.0 | 2.3−25.0 | 2.2−25.0 | 2.7−25.0 |
| crystal size/mm | 0.5 × 0.4 × 0.3 | 0.35 × 0.3 × 0.2 | 0.3 × 0.3 × 0.3 | 0.4 × 0.4 × 0.4 | 0.6 × 0.3 × 0.2 |
| no. of data collected | 4527 | 4165 | 3290 | 3072 | 2550 |
| no. of unique data | 4274 | 3905 | 2808 | 2858 | 2161 |
| *hkl* range | −1→14; −15→2; −2→25 | −2→14; −2→18; −19→2 | −9→9; −19→2; −1→12 | −1→14; −15→2; −2→16 | −9→1; −15→2; −2→17 |
| $R_{int}$ | 0.05 | 0.015 | 0.010 | 0.025 | 0.0225 |
| standard reflections | (−4−5 1) (−3 3 7) (−4 3−6) | (3 5 5) (4 5−3) (−4 5 3) | (−2 5 3) (−3 2−3) (2 6−3) | (−3−5 3) (−1−1 7) (0 6 2) | n/a |
| no. of data in refinement | 4272 | 3904 | 2808 | 2858 | 2160 |
| no. of refined parameters | 321 | 294 | 299 | 259 | 195 |
| final $R$ [$I > 2\sigma(I)$] (all data)[a] | 0.062 (0.118) | 0.042 (0.074) | 0.030 (0.032) | 0.029 (0.035) | 0.022 (0.022) |
| w$R2$ [$I > 2\sigma(I)$] (all data) | 0.145 (0.172) | 0.105 (0.115) | 0.084 (0.085) | 0.075 (0.079) | 0.061 (0.061) |
| goodness of fit $S$ | 0.893 | 0.95 | 1.073 | 1.064 | 1.129 |
| flack absolute structure parameter | 0.03 (3) | 0.04(2) | 0.02(2) | −0.05(5) | 0.00(4) |
| largest remaining feature in electron density map/eÅ$^{-3}$ | 0.50 (max) | 0.27 (max) | 0.50 (max) | 0.43 (max) | 0.36 (max) |
| | −0.30 (min) | −0.22 (min) | −0.23 (min) | −0.71 (min) | −0.30 (min) |
| shift/esd in last cycle (max) | 0.002 | 0.001 | 0.003 | 0.001 | n/a |

[a] $R = \Sigma(|F_o| - |F_c|)/\Sigma(F_o)$. $wR2 = \{\Sigma[w(F_o^2 - F_c^2)^2]/\Sigma[w(F_o^2)^2]\}^{1/2}$. $R_{int} = \Sigma|F_o^2 - F_o^2(\text{mean})|/\Sigma F_o^2$ (summation is carried out only where more than one symmetry equivalent is averaged). [b] Some data items for structure **5** are not available (see text).

the $\psi$-scan data that were collected indicated that no absorption correction was necessary. All structures were solved by direct methods (SIR92).[15] All non-H atoms were allowed anisotropic thermal motion. Phenyl groups were refined as rigid idealized hexagons with C−C =1.39 Å. Aliphatic CH hydrogen atoms were included at calculated positions, with C−H = 0.96 Å. For complex **1** the two OH hydrogen were found from difference Fourier maps and refined with fixed positions. For complex **2** the OH positions could not be obtained, and these hydrogens were not included in the model. Refinement (SHELXL93)[16] was by full-matrix least-squares on $F^2$, using all the unique data and the weighting scheme $w = [\sigma^2(F_o)^2 + (AP)^2 + BP]^{-1}$ where $P = [F_o^2/3 + 2F_c^2/3]$. For molecule **1**, A = 0.0952, B = 0.0; for molecule **2**, A = 0.0696, B = 0.0; for molecule **3**, A = 0.0581, B = 0.2225; for molecule **4**, A = 0.0441, B = 0.7298. The archive computer file for complex **5** became corrupted, so that some (less essential) data items for **5** are not available. $\sigma(F_o)^2$ was estimated from counting statistics. Neutral atom scattering factors, coefficients of anomalous dispersion, and absorption coefficients were obtained from ref 17. The absolute configurations for complexes **1**−**5** were confirmed by the refinement of the Flack absolute structure parameter, which refined to zero within error for all data sets. Complexes **1** and **2** both contained ethanol of solvation. Complex **1** contained two independent molecules of ethanol; one molecule could be satisfactorily refined, whereas the other was heavily disordered. The SQUEEZE procedure in PLATON[18] was applied to compensate for this disordered molecule. For molecule **2**, calculations using PLATON[18] indicated that there was a void in the lattice that probably contained a disordered half-molecule of ethanol, but this solvent was not included in the model. All calculations were carried out on a Pentium P120 PC, and all thermal ellipsoid plots were obtained using the program PLATON.[18]

**Acknowledgment.** The authors gratefully acknowledge the support of the EPSRC (Process Engineering Separations Initiative; grant number GR/J 45190).

**Supporting Information Available:** Complete tables of crystallographic data, final atomic coordinates, bond lengths and angles, anisotropic displacement parameters, and hydrogen coordinates for compounds **1**−**5**; infrared and NMR spectroscopic data on the new compounds. This material is available free of charge via the Internet at http://pubs.acs.org.

IC980172L

---

(14) Walker, N.; Stuart, D. *Acta Crystallogr., Sect. A* **1983**, *A39*, 158−166.

(15) Altomare, A.; Cascarno, G.; Giacovazzo, C.; Gualiardi, A. Sir92−A Program for Automatic Solution of Crystal Structures by Direct Methods. *J. Appl. Crystallogr.* **1994**, *27*, 435.

(16) Sheldrick, G. M. *SHELXL93: A Program for Crystal Structure Refinement*; University of Göttingen: Germany, 1993.

(17) Tables 4.2.4.2, 4.2.6.8, and 6.1.1.4 from *International Tables for Crystallography, Vol. C, Mathematical, Physical and Chemical Tables*; Kluwer: Dordrecht, 1995.

(18) Spek, A. L. PLATON. *Acta Crystallogr., Sect. A* **1990**, *A46*, C34.